Nature of Grain Refinement in Titanium Alloy Welds by Microcooler Inoculation

Fine equiaxed grains were observed throughout the fusion zone of GTA welds inoculated with Ti-6Al-4V powder

BY D. L. HALLUM AND W. A. BAESLACK III

ABSTRACT. The influence of microcooler inoculation on the solidification and fusion zone beta grain structure of gas tungsten-arc welds in titanium has been investigated by the addition of Ti-6Al-4V powder to the weld pool in Ti-15V-3Al-3Cr-3Sn sheet. The complete melting of a large proportion of the added powder particles effectively lowered the fusion zone melt temperature and reduced temperature gradients across this region, thereby promoting the growth of equiaxed dendrites both from partially melted powder particles and in a more conventional manner from dendrite fragments. The equiaxed dendrites subsequently blocked the growth of epitaxially nucleated columnar grains throughout a large portion of the fusion zone. The fine, equiaxed beta grain structure exhibited within the fusion zone at room temperature differed markedly from the beta grain structure that existed at the completion of solidification due to appreciable grain boundary migration and possible dynamic recrystallization during cooling through the beta phase field. Powder additions to gas tungsten arc (GTA) welds in Ti-6Al-4V sheet promoted a similar, predominantly equiaxed fusion zone beta grain morphology. The simultaneous application of EMS at a moderate field strength during welding with powder additions reduced the extent of grain refinement.

Introduction

Origin of the Fusion Zone Grain Structure in Titanium Alloy Welds

Fusion welds in titanium alloys are characterized by coarse, columnar-shaped beta grains in the fusion zone (FZ). As schematically illustrated in Fig. 1 for an elliptical-shaped weld pool in titanium sheet, these grains nucleate epitaxially upon coarsened beta grains in the near heat-affected zone (NHAZ) and grow competitively into the molten weld pool. During this competitive growth process, grains whose preferred growth directions (< 100> type in BCC beta titanium) are most favorably oriented with respect to the maximum temperature gradient across their solid-liquid interface grow at the expense of less favorably oriented grains, thereby promoting the formation of a coarse, columnar FZ grain structure (Ref. 2). The presence of a continuous beta grain growing along the FZ centerline is also common in elliptical-shaped weld pools in titanium sheet. This grain forms when the preferred growth direction of a columnar grain becomes parallel to the direction of the maximum temperature gradient at the tail end of the weld pool (which coincides with the welding direction). The presence of coarse FZ beta grains, which in thin sheet may completely traverse the FZ thickness, can be particularly detrimental in alpha-beta titanium alloys in which continuous alpha (the low-temperature HCP phase in titanium) at prior-beta grain boundaries provides preferential paths for intergranular fracture at low ductility (Ref. 3).

The FZ beta grain structure in titanium alloy welds is dependent on several factors, including: 1) the thermal cycle in the NHAZ as it influences the growth and ultimate size of the beta grains from which FZ grains grow; 2) the shape of the weld pool due to its influence on the competitive grain growth process; and 3) the cooling rates experienced during solidification. In most titanium welding applications these factors, and therefore the FZ beta grain size, are determined principally by the weld energy input. In general, a reduction in grain size is accomplished by

KEY WORDS

Titanium Alloy
Grain Refinement
Microcooler Inoculation
Fusion Zone
Fusion Welds
Dendrite Fragmentation
Heterogeneous Nucleation
Solidification Behavior
Grain Growth
Grain Morphology

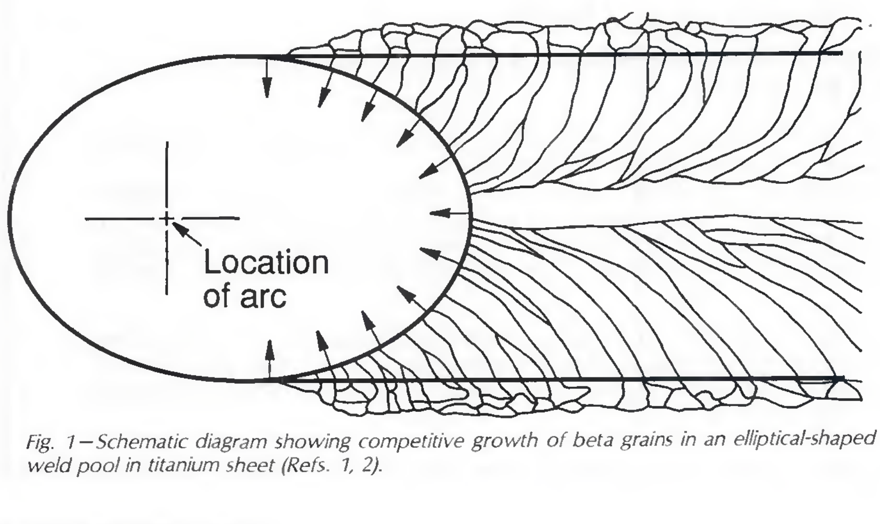

Fig. 1 — Schematic diagram showing competitive growth of beta grains in an elliptical-shaped weld pool in titanium sheet (Refs. 1, 2).

D. L. HALLUM is with Carleton Technology Inc.,Orchard Park, N.Y.W. A. BAESLACK III is with the Department of Welding Engineering, The Ohio State University, Columbus, Ohio.

decreasing the energy input through modification of the welding parameters or the utilization of an alternate welding process (*e.g.*, substitution of GTA welding with laser or electron beam welding) (Ref. 4). Unfortunately, lower weld energy inputs are also associated with higher cooling rates, which can promote the formation of brittle, martensitic microstructures in many alpha-beta titanium alloys. Thus, potential improvements in the ductility of low-energy-input welds due to a reduced beta grain size may be offset by the formation of a more brittle intragranular microstructure.

Grain Refinement in Titanium Alloy Welds

In the past, numerous investigators have examined the potential for grain refinement in titanium alloy welds using electromagnetic stirring (EMS), inoculation techniques or a combination of these two methods. EMS generally involves the application of an alternating, longitudinal electromagnetic field (*i.e.*, coaxial with the welding torch) to promote fluid flow and agitation of the weld pool. Early studies by Brown, *et al.* (Ref. 5), showed that the application of EMS during GTA welding promoted appreciable FZ grain refinement in Ti-6Al-4V, but was relatively ineffective in refining the grain size in the metastable-beta alloy Ti-13V-11Cr-3Al. Soviet investigators subsequently demonstrated the advantages of EMS in improving the mechanical and corrosion properties of welds in pure titanium and titanium alloys (Refs. 6–11). Boldyrev, *et al.* (Ref. 6), showed the capability of EMS to refine the FZ beta grain structure in titanium alloy welds and thereby, potentially improve mechanical properties, although he noted that the grain-refining effect was less than that observed in austenitic stainless steel. EMS was also found to enhance weld properties in titanium by improving the transformed-beta microstructure (Ref. 7), reducing porosity (Ref. 8) and promoting a refined solidification substructure (Ref. 10). In contrast to these earlier results, recent work by DeNale, *et al.* (Ref. 12), determined EMS using a transverse electromagnetic field to be essentially ineffective in altering the FZ beta grain structure of GTA welds in Ti-6Al-4V.

The limited effectiveness of EMS in promoting weld FZ grain refinement in titanium alloys, as compared to other alloy systems, can be explained by considering the principal mechanism of grain refinement reportedly operative during EMS. The early work of Brown, *et al.* (Ref. 5), on titanium, and Bolydrev, *et al.* (Ref. 6), on titanium and stainless steel, and more recent studies by Matsuda, *et al.*, on aluminum and stainless steel (Refs. 13, 14) and Kou and Le on aluminum (Ref. 15), indicate that FZ grain refinement during EMS results primarily from the fragmentation of cellular-dendrite arms or columnar-dendrite tips at the solid-liquid interface. In contrast to aluminum alloys and many stainless steels, most commercial titanium alloys are characterized by a relatively narrow solidification range (or more precisely, a narrow region of constitutional supercooling in the liquid ahead of the FZ solid-liquid interface). Grain refinement by dendrite-tip fragmentation in titanium alloys is therefore difficult due to the narrow "mushy zone" into which the dendrites protrude. Abrolov, *et al.* (Ref. 16), directly observed the advancing solid-liquid interface in commercially pure titanium during EMS and found a complete absence of dendrite fragmentation or heterogeneous nucleation ahead of the advancing interface. This was attributed primarily to solidification by planar and cellular rather than dendritic growth, which is not unexpected considering the low solute content of this alloy. More highly alloyed titanium alloys might be expected to exhibit increasingly dendritic solidification and a wider solidification range, and therefore a greater potential for dendrite fragmentation. However, the aforementioned work of DeNale, *et al.* (Ref. 12), on GTA welds in Ti-6Al-4V concurred with that of Abrolov in indicating difficulties in the promotion of dendrite fragmentation and beta grain refinement due to the narrow constitutionally supercooled region at the weld solid-liquid interface. The inability by Brown, *et al.* (Ref. 5), to achieve grain refinement by EMS in Ti-13V-11Cr-3Al, which exhibits a comparatively wide solidification range due its high alloying content, further confirms the difficulties in inhibiting epitaxial nucleation and columnar grain growth even in titanium alloys most likely to experience dendrite fragmentation. Despite these limitations in promoting equiaxed grain nucleation and growth in titanium welds, it should be noted that EMS may also influence the fusion zone beta grain size and morphology by altering the thermal conditions and macro solidification behavior of the weld pool (*i.e.*, the weld pool shape and size), thereby influencing competitive growth between epitaxially nucleated FZ beta grains.

Attempts to promote FZ grain refinement in titanium alloy welds by inoculation with refractory particles have involved the addition of yttrium to the weld pool, which reportedly forms a high melting point Y_2O_3 oxide (yttria) via in-situ oxidation (Refs. 17–19). Initial studies by Simpson (Ref. 17) found that although the addition of yttrium to GTA welds in Ti-6Al-6V-2Sn did not prevent epitaxial growth, it did promote a finer, more equiaxed grain structure near the FZ centerline. He attributed this refinement to a drag effect of the fine yttria particles on the advancing solid-liquid interface that allowed heterogeneous nucleation of beta grains in the final liquid to solidify. Misra, *et al.* (Ref. 18), showed similar grain refinement effects in Ti-6Al-4V, but alternatively suggested that yttrium additions result in grain refinement by a combination of the heterogeneous nucleation of beta grains on yttria particles combined with a favorable change in beta grain-growth kinetics. A subsequent analysis by Nordin, *et al.* (Ref. 19), concluded that yttrium additions refine the FZ beta grain size of GTA welds in Ti-6Al-2V-1Mo-1Nb by altering the weld pool fluid flow and the thermal conditions and, as suggested by Misra, *et al.*, providing heterogeneous nucleation sites in the form of yttria. Although supported by quantitative measurements of beta grain size, neither of these latter two studies provides definitive evidence for heterogeneous nucleation, and thus, the exact mechanism by which yttrium promotes grain refinement remains unclear.

An early study by Ivochkin (Ref. 20) demonstrated that columnar grain growth in the FZ of GTA welds in high-strength steel can be inhibited by the addition of low-carbon steel powder to the trailing edge of the weld pool. He proposed that the powder particles remove superheat from the weld pool and supercool localized regions in the liquid. Equiaxed grains subsequently nucleate both at these "freezing centers" and from partially melted powder particles. The growth of these equiaxed grains in the molten weld pool ahead of the macroscopic solid-liquid interface blocks the growth of columnar grains which nucleate epitaxially at the fusion line. A subsequent theoretical analysis of Ivochkin's work by Shamanin (Ref. 21) proposed that equiaxed grain formation results principally from nucleation on unmelted powder particles in the cooled liquid, rather than from nucleation within the melt at regions of local supercooling. He also modified Ivochkin's formula for predicting the quantity of powder required to suppress columnar growth, which was based on an unrealistic requirement of removing superheat from the entire weld pool, and indicated that the prediction of optimum powder additions could not be determined strictly from theoretical considerations.

Following the work of Ivochkin, studies by Boldyrev, *et al.* (Refs. 6, 22 and 23), showed that the addition of small titanium and/or zirconium particles, called "microcoolers" or "modifiers," to the weld pool can promote grain refinement in thin-sheet titanium-alloy welds. These particles, which were 0.3 to 0.6 mm (0.012 to 0.024 in.) in diameter, were added to the trailing edge of the weld pool and reportedly displaced by EMS in a uniform manner to the solid-liquid interface. Furthermore, although these investigators showed that microcooler additions improve the weld mechanical and corrosion properties, they did not discuss the quantitative extent of

Table 1—GTA Welding Process Parameters

Welding Parameters/ Conditions[(a)]	Phase I	Phase II	
Base metal	Ti-15-3	Ti-15-3	Ti-6-4
Welding current (A)	60	55	75
Arc voltage (V)	11.5, DCEN	10, DCEN	
Inert gas shielding, L/min (ft^3/h)	Argon chamber-4.8 (10)[(b)] torch-12 (25) trailing-5.5 (12) backing-13.6 (30)	Argon chamber-4.8 (10) torch-12 (25) trailing-5.5 (12) backing-13.6 (30)	
Travel rate, mm/s (in./min)	2.5 (6)	2.1 (5)	
Powder sizes,[(c)] mm (in.)	Fine, Coarse	Coarse	
Powder feed rate, (g/s)	0.045, 0.055 for fine 0.045, 0.080 for coarse	0.055 for coarse	
Magnetic field, longitudinal, gauss	—	50 gauss (3 Hz)	

(a) 2.4-mm (0.093-in.) diameter 2% thoriated-tungsten electrode, 2-mm (0.125-in.) radius, conical tip.
(b) Welding chamber was purged at 18 L/min (40 ft^3/h) for three min prior to welding.
(c) Fine powder: 0.149 to 0.208 mm (0.0059 to 0.0082 in.) diameter. Coarse powder: 0.208 to 0.295 mm (0.0082 to 0.0116 in.) diameter.

grain refinement or the specific nature and mechanism of this grain refinement process for titanium alloys.

Objective and Approach

The overall objective of the present work was to determine the influence of microcooler inoculation on the solidification behavior and evolution of the beta grain structure in GTA welded titanium sheet. This was accomplished by the inoculation of GTA welds in the metastable-beta titanium alloy Ti-15V-3Al-3Cr-3Sn (hereafter designated as Ti-15-3) sheet with powder produced from the alpha-beta titanium alloy Ti-6Al-4V (hereafter designated as Ti-6-4). Previous GTA welding studies on Ti-15-3 (Ref. 24) had shown that rapid cooling rates promote retention of the high-temperature beta phase down to room temperature. Consequently, the utilization of a Ti-6-4 powder inoculant, which exhibits a fine, transformed-beta (*i.e.*, alpha and/or alpha-prime) microstructure on rapid weld cooling, allowed the location of the individual powder particles within the FZ to be observed in a manner not possible with a similar particle/matrix combination. In addition, clear resolution of the dendritic solidification substructure in the retained-beta FZ matrix allowed analysis of the weld solidification behavior. Such analysis would not be possible in welds exhibiting a completely transformed-beta microstructure. Following this mechanistic study, the effectiveness of Ti-6-4 powder additions in refining grains in GTA welded Ti-15-3 and Ti-6-4 sheets was evaluated with and without the simultaneous application of EMS.

Experimental Procedure

Materials

Ti-15-3 and Ti-6-4 sheet materials 1.27 mm (0.05 in.) and 1.58 mm (0.0625 in.) in thickness, respectively, were sectioned into weld coupons 152 to 203 mm (6.0 to 8.0 in.) in length and 25.4 (1.0 in.) in width. Prior to GTA welding, the sheet surfaces were ground with 320-grit SiC paper and pickled in a solution of 3 vol-% HF + 6 vol-% HNO_3 + 91 vol-% H_2O for approximately one minute, rinsed in water and acetone, and dried.

Spherical Ti-6-4 powder was produced using the rotating-electrode process (REP). As shown in Fig. 2, this process produced a wide range of powder particle sizes. In order to assess powder particle size on grain refinement, the powder was sieved to provide particle size ranges of the following: 1) 0.295 to 0.208 mm diameter (0.0116 to 0.0082 in.); and 2) 0.208 to 0.149 mm (0.0082 to 0.0059 in.). In this paper, these two powder particle sizes are designated as coarse and fine, respectively. It should be noted that these particles were somewhat finer than the 0.3 to 0.6-mm (0.012 to 0.024-in.) diameter microcoolers employed by previous investigators (Refs. 6, 22, 23).

Gas Tungsten Arc Welding

Bead-on-plate GTA welds were produced using an apparatus similar to that previously employed by Boldyrev, *et al.* (Refs. 6, 24, 25)—Fig. 3. Welding parameters shown in Table 1 were controlled to provide full penetration with nearly equal top and bottom weld pool widths (ap-

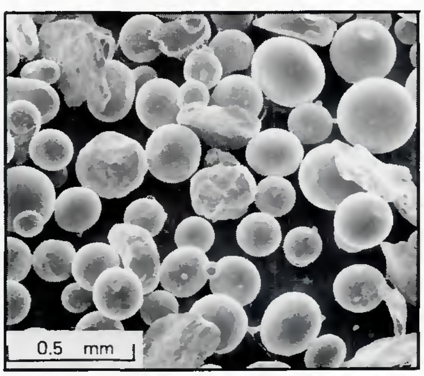

Fig. 2—Scanning electron micrograph of Ti-6-4 powder produced by rotating-electrode process.

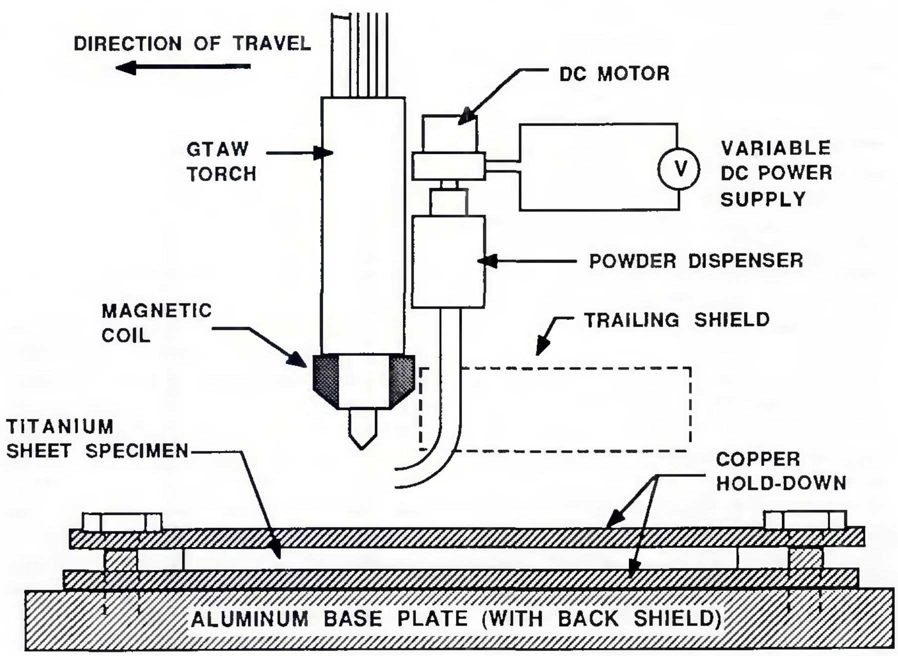

Fig. 3—Schematic illustration of experimental apparatus used for GTA welding of titanium sheet with powder additions and EMS. Welding torch, powder feeding apparatus and fixture were enclosed within an argon-purged Plexiglas chamber.

proximately 8 mm/0.31 in.) and an elliptical-shaped weld pool to facilitate powder addition across the weld width. Welding was performed in a Plexiglas chamber purged with high-purity argon to prevent atmospheric contamination. Additional shielding was provided by the flow of high-purity argon through the welding torch, a trailing shield and the aluminum backing fixture. Powder was added to the trailing edge of the weld pool using an auger feed screw device driven by a DC motor. The powder-dispensing device exhibited a flared tip approximately 5 mm (0.2 in.) in width in order to uniformly distribute powder across the weld pool width, and was positioned approximately 4.0 mm (0.16 in.) above and 2 mm (0.08 in.) ahead of the trailing edge of the weld pool. Powder feed rates were selected based on requirements to maximize the quantity of powder deposited into the molten weld pool without influencing arc or process stability and minimize the quantity of residual partially adhered or loose powder on the weld surface. The as-welded top surface of a weld produced in Ti-15-3 with coarse powder at a feed rate 0.080 g/min exhibits an irregular topography (Fig. 4) and the presence of adhered powder particles. Welds produced with finer powder and at lower feed rates generally exhibited a smoother surface, but still showed the same adherence of powder particles.

In Phase I of the study, the influence of powder size and feed rate on the quantitative extent and nature of grain refinement in GTA welded Ti-15-3 was investigated. At least three welds were produced and evaluated for each combination of welding parameters. In Phase II, Ti-6-4 microcooler additions were added to GTA weld pools in both Ti-15-3 and Ti-6-4 sheet using a powder size and feed rate optimized from Phase I (Table 1) with and without the application of a longitudinal electromagnetic field. A reversing (3 Hz) longitudinal magnetic field of 50 gauss (measured across the arc gap) was generated by a coil mounted coaxially with the gas cup of the welding torch. The tip of the coil was located 5 mm (0.02 in.) above the weld surface. In Phase II, only one weld was produced per condition.

Weld Characterization

Subsequent to welding, coupons were sectioned using a diamond saw and mounted in epoxy for microstructure and grain size analysis. After grinding down with 600-grit SiC paper, the specimens were polished with 0.05-micron alumina and etched using Kroll's reagent.

Grain size analysis was conducted on all specimens using a standard line-intercept method. Grain sizes were measured on the top and bottom weld FZ surfaces in directions normal and parallel to the welding direction, and transverse through the FZ thickness. Since the FZ exhibited regions of both columnar and equiaxed grain morphologies, measurements parallel to the welding direction were made individually in both structures. Proportions of equiaxed vs. columnar grain regions were also determined to within ±5%. It should be noted that at least three measurements were made for each specimen/orientation combination and averaged. The influence of grain refinement on mechanical properties was analyzed for the Ti-6-4 welds by the three-point bend testing of longitudinal-weld-oriented specimens. Fractographic examination of the bend specimen fracture surfaces was performed using scanning electron microscopy.

Results

Phase I—Ti-6-4 Powder/Ti-15-3 Sheet Welds

Table 2 summarizes FZ beta grain size measurements for the top and bottom surfaces and transverse sections through the thickness of each weld. As indicated, the FZ grain sizes of welds produced with powder additions measured parallel to the welding direction included those in both equiaxed and columnar regions. Grain size measurements perpendicular to the welding direction reflected both the average sizes of each grain morphology and also

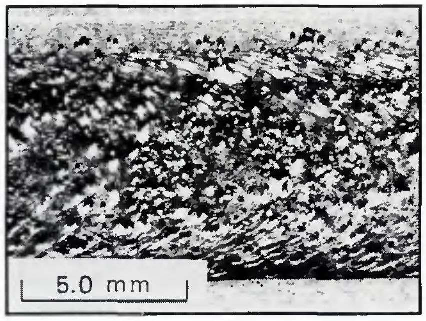

Fig. 4—As-welded top surface of GTA weld in Ti-15-3 produced with addition of coarse-diameter Ti-6-4 powder at rate of 0.080 g/min. Arrow indicates welding direction.

Table 2—Quantitative Grain Size Measurements for GTA Welds in Ti-15-3 and Ti-6-4(a)

Base Alloy	Powder Size (mm)	Feed Rate (g/min)	Grain Size (mm) Top Trans.	Top Long. Eq.	Top Long. Col.	Eq./Col. Ratio
			Phase I			
Ti-15-3	—	—	0.65	—	0.56	0/100
Ti-15-3	F	0.045	0.17	0.15	0.28	70/30
Ti-15-3	F	0.055	0.17	0.14	0.31	75/25
Ti-15-3	C	0.045	0.16	0.14	0.25	85/15
Ti-15-3	C	0.080	0.16	0.15	0.27	85/15
			Phase II			
Ti-15-3	—	—	0.48	—	0.50	0/100
Ti-15-3	C	0.055	0.16	0.14	0.23	85/15
Ti-15-3M	C	0.055	0.38	—	0.30	10/90
Ti-6-4	—	—	0.76	—	0.82	0/100
Ti-6-4	C	0.055	0.28	0.23	0.36	80/20
Ti-6-4M	—	—	0.65	—	0.68	0/100
Ti-6-4M	C	0.055	0.32	0.27	0.47	70/30

Grain Size (mm) Bottom Trans.	Bottom Long. Eq.	Bottom Long. Col.	Bottom Eq./Col. Ratio	Through Thickness Eq.	Through Thickness Col.
			Phase I		
1.10	—	0.45	0/100	—	0.42
0.29	0.21	0.32	60/40	0.14	0.29
0.25	0.23	0.34	60/40	0.14	0.31
0.24	0.19	0.29	60/40	0.15	0.21
0.27	0.22	0.28	60/40	0.16	0.31
			Phase II		
1.12	—	0.41	0/100	—	0.39
ND	ND	ND	ND	0.17	0.32
0.61	—	0.43	0/100	—	0.29
0.76	—	0.49	0/100	—	0.36
0.36	0.30	0.43	60/40	0.23	0.31
0.77	—	0.53	0/100	—	0.39
0.55	—	0.44	0/100	—	0.35

(a) Tvs.—FZ grain size measured perpendicular to welding direction.
Long.—FZ grain size oriented parallel to welding direction.
Eq.—Equiaxed grains; Col.—Columnar grains.
M—Applied longitudinal magnetic field, 50 gauss, 3 Hz.

the proportions of each morphology across the FZ.

The macroscopic beta grain structure exhibited by the autogenous "control" weld in Ti-15-3 closely resembled that of the schematic illustration in Fig. 1. Figures 5A–C show control weld grain structures from the NHAZ to the FZ centerline on the top and bottom surfaces and in a cross-section through the thickness perpendicular to the welding direction, respectively. Consistent with the previous discussion, the FZ exhibited coarse, columnar beta grains which nucleated upon coarsened beta grains in the NHAZ and grew in toward the center of the molten weld pool. As growth proceeded, the average columnar grain width increased from approximately 0.25 mm (0.010 in.) at the weld fusion line to a maximum of about 0.56 mm (0.022 in.) near the FZ centerline. The elliptical pool shape also promoted the formation of coarse, centerline grains 1–2 mm (0.039-0.078 in.) in width, which grew for distances of up to several millimeters. The beta grain morphology on the bottom side of the weld was similar to that of the top surface. However, a much larger proportion of the weld pool width solidified to one or two wide centerline grains (up to 3 mm/0.12 in. in width) which grew along the entire weld length. The transverse section shown in Fig. 5C shows the coarse, columnar grain growth from the NHAZ in toward the weld centerline, and the coarse beta grain at the bottom-center of the FZ. Note that at the center of the FZ, the entire FZ was only two beta grains in thickness. From the orientation of the cellular-dendritic solidification substructure, it is apparent that the grains near the fusion boundary grew primarily in toward the centerline and then up toward the top surface. Furthermore, the observation of a "Maltese cross" cellular-dendritic solidification substructure in the wide, centerline grain on the top surface (Fig. 5A) indicates that the growth of this grain occurred both along the weld length and up toward the top surface.

The addition of powder to the trailing edge of the weld pool significantly modified the FZ beta grain structure as compared to the autogenous weld. Figure 6A shows the top surface of a weld produced with fine powder at a feed rate of 0.045 g/min. Although epitaxial nucleation was not prevented, only limited columnar grain growth was observed near the fusion boundary. The narrower width of these columnar grains, as compared to those in the control weld (0.28 vs. 0.56 mm/0.011 vs. 0.022 in.), resulted from the shorter distance over which competitive growth could occur before the grains impinged equiaxed grains solidifying in the weld pool ahead of the macroscopic solid-liquid interface. As shown in Fig. 6A, the columnar zone transitioned to a central region of equiaxed beta grains. Also evident on the top surface were numerous unmelted powder particles of varying sizes distributed both uniformly across the equiaxed region of the FZ surface and occasionally in clusters. Although powder particles were occasionally located at the centers of the beta grains, observation at higher magnification (Fig. 6B) showed that the beta grain boundaries frequently traversed powder particles.

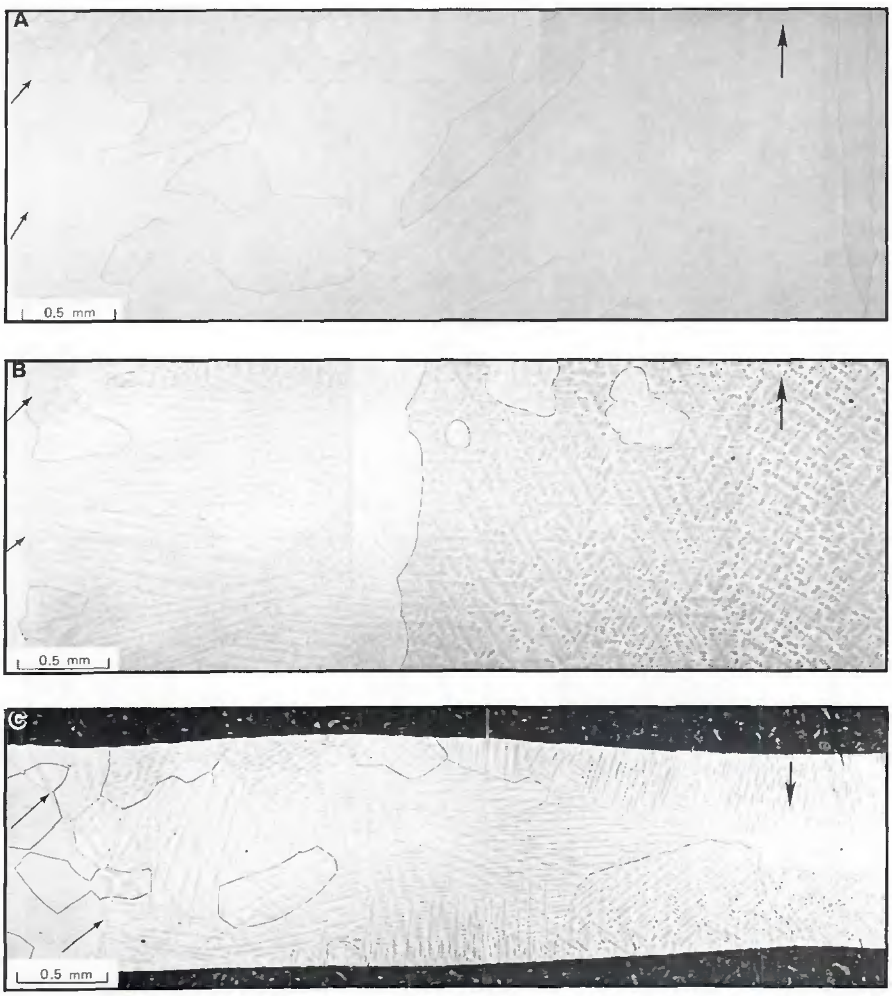

Fig. 5 — Light micrographs of autogenous GTA weld in Ti-15-3 sheet: A — top surface; B — bottom surface; C — transverse, through-thickness cross-section. Large arrow indicates FZ centerline and/or welding direction, small arrows indicate fusion line.

Heavy etching of the specimen clearly delineated the solidification substructure. As evident in Figs. 6A and B, the partially melted powder particles served as nucleation sites for equiaxed dendrites. The size of the powder particles that served as these nuclei varied from nearly the original particle size to less than one-tenth of this size. These variations were attributed to differing thermal excursions experienced by powder particles in the molten weld pool. As shown in Fig. 6B, equiaxed-dendritic beta grains grew from these particles (which transformed entirely to beta phase on heating in the molten weld pool) to a diameter ranging from about two to five times the original powder particle diameter. The equiaxed vs. columnar morphology of these heterogeneously nucleated grains resulted from the effect of the powder particles (including those both partially and completely melted) in effectively cooling the weld pool liquid and minimizing temperature gradients which would normally promote columnar growth. Throughout the central 70% of the FZ, the equiaxed dendrites consumed the FZ liquid and ultimately impinged upon each other. However, near the fusion boundary, where powder particles were less dense, regions between the powder particles solidified as columnar grains across the macroscopic solid-liquid weld pool interface. Occasionally, the isolated powder particles in this region actually served as the nuclei for a columnar grain.

The absence of a correlation between the irregular solidification beta grain boundaries of the equiaxed dendrites and the relatively straight beta grain boundaries present at room temperature indicated the occurrence of appreciable beta grain migration during cooling. The higher density of equiaxed beta grains vs. the powder particles and equiaxed dendrites was of particular interest, and further suggests the dynamic recrystallization of the beta grain structure on cooling.

Quantitatively, the average equiaxed grain size of 0.15 mm (0.0059 in.) on the FZ top surface was appreciably finer than the columnar grain size of 0.56 mm (0.022 in.) and the coarse centerline grain size of 1–2 mm (0.039–0.078 in.) in width in the autogenous weld.

Fig. 6C shows the transverse, through-thickness section of a weld produced with fine powder at a feed rate of 0.045 g/min. Weld reinforcement was maximum in the central region of the FZ (about 25% of the sheet thickness) and gradually decreased toward the fusion lines. The average reinforcement of about 10% correlated well with values calculated from powder deposition rates. It is of interest to note that a relatively small proportion, perhaps as low as 10 to 20% by volume, of the powder particles actually survived to ultimately serve as nucleation sites. The majority of the powder particles melted and effectively cooled the molten weld pool, thereby allowing equiaxed growth of surviving particles. As on the top surface, the steeper temperature gradients and lower concentration of powder particles near the fusion boundaries allowed the limited growth of columnar grains in these regions. However, throughout most of the FZ, relatively fine, equiaxed beta grains were observed. In contrast to the top surface, actual powder particles were not dispersed throughout the equiaxed beta grains, and were numerous only near the top surface. However, the equiaxed-dendrite and migrated beta grain structures throughout this cross-section were quite similar in size and morphology to those observed on the top surface. This observation strongly suggests that equiaxed-dendrite growth in this region also occurs from broken dendrite tips present in the liquid, and not only from unmelted powder particles. An average grain size of 0.14 mm (0.0055 in.) in the equiaxed region across the thickness of the transverse section was almost identical to that on the top surface.

Figure 6D shows the bottom surface of the GTA weld produced with fine powder at 0.045 g/min. The small number of powder particles present during solidification at the bottom of the weld pool promoted less equiaxed-dendrite growth and a lower proportion of equiaxed vs. columnar grains (60/40) than on the top surface. Although formation of the centerline grain that dominated the autogenous control weld FZ structure was prevented, occasional epitaxially nucleated columnar grains were observed. Correspondingly, the average beta grain size of 0.21 mm (0.0026 in.) was greater than that on the FZ top surface or through thickness.

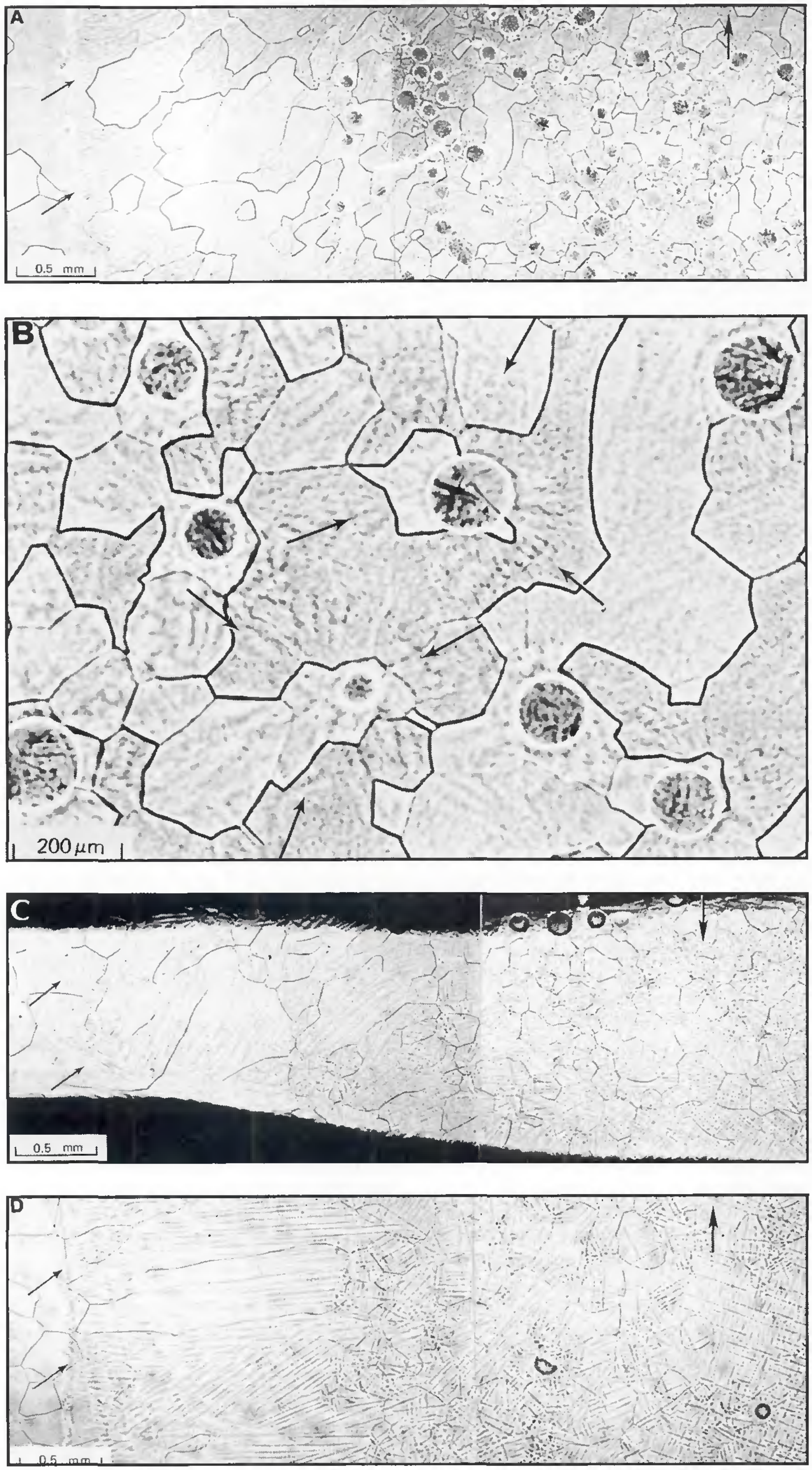

Fig. 6 — Light micrographs of GTA weld in Ti-15-3 sheet produced with addition of fine-diameter Ti-6-4 powder at a rate of 0.045 g/min: A — top surface; B — top surface at increased magnification, arrows indicate solidification grain boundaries; C — transverse, through-thickness cross-section; D — bottom surface. Large arrows in A, C, and D indicate FZ centerline and/or welding direction, small arrows indicate approximate fusion line.

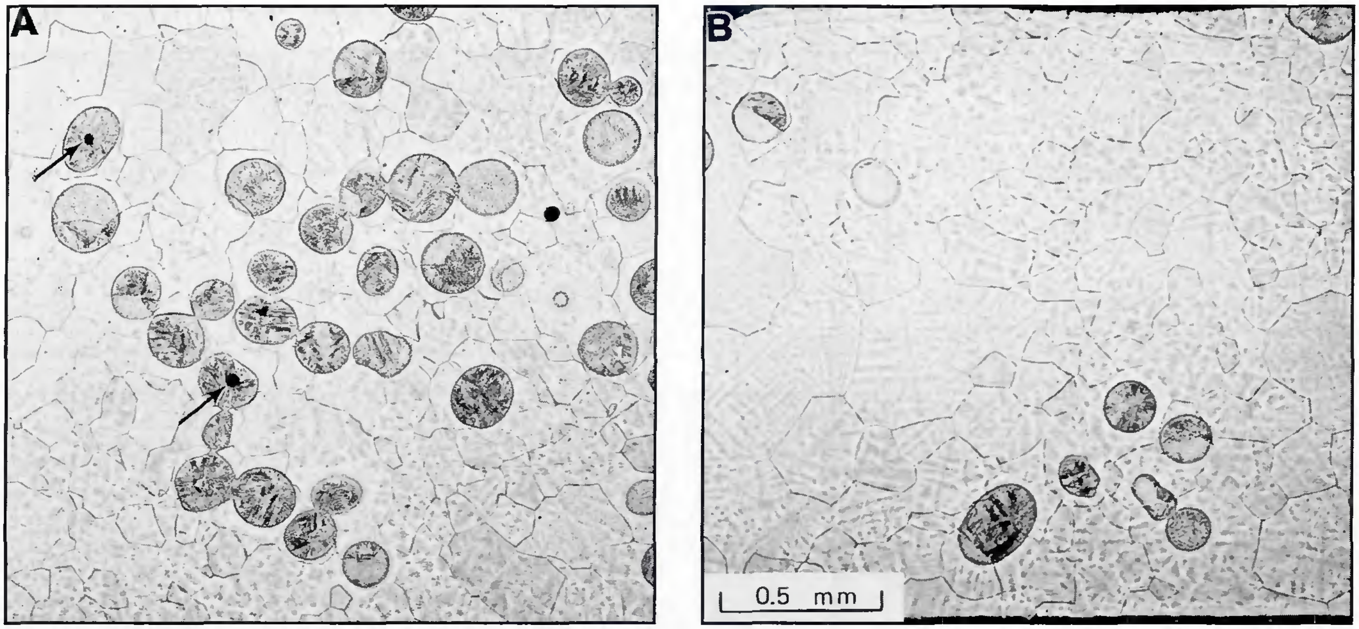

Fig. 7 — Light micrographs of GTA weld in Ti-15-3 sheet produced with addition of coarse-diameter Ti-6-4 powder at a rate of 0.45 g/min: A — FZ center on top surface; B — FZ center on transverse, through-thickness cross-section; Arrows in A indicate fine pores at center of occasional coarse powder particles.

As shown in Table 2, an increase in the powder feed rate for the fine powder from 0.045 to 0.055 g/min promoted minimal change in the FZ beta grain morphology or grain size, although it did slightly increase the proportion of equiaxed vs. columnar beta grains on the FZ surface. In contrast, the use of coarser powder particles at moderate and high powder feed rates generally promoted a greater proportion of equiaxed vs. columnar grains both on the top surface and throughout a significant portion of the FZ. Figure 7A shows the FZ center on the top surface of a weld produced with coarse powder at a feed rate of 0.045 g/min. As expected, the average size of the partially melted powder particles was greater than observed in Fig. 6A for the weld produced with fine powder. In addition, the extent of columnar grain growth at the fusion boundary was negligible, with epitaxially nucleated grains appearing nearly equiaxed. This observation of minimal columnar growth near the top surface was consistent with an average columnar grain size of about 0.26 mm (0.010 in.) vs. 0.29 mm (0.011 in.) for welds produced with the coarse vs. the fine powder, respectively. Also observable in Fig. 7A are the occasional presence of fine pores or shrinkage cavities at the center of coarser powder particles.

Figure 7B shows the FZ center in a transverse, through-thickness cross-section of a weld produced with coarse powder at a feed rate of 0.045 g/min. This structure, and that of the bottom FZ surface, generally appeared similar to those produced with finer powder, although the equiaxed grain structures were more uniform and a greater number of larger powder particles were somewhat randomly observed near the center and bottom portions of the FZ. The inability to significantly increase the proportion of equiaxed vs. columnar grains with increased powder diameter and feed rate was indicative of the aforementioned limitations and difficulties associated with effectively distributing the powder across the entire weld pool solid-liquid interface.

Phase II—Ti-6-4 Powder/Ti-15-3 and Ti-6-4 Powder/Ti-6-4 Sheet Welds with EMS

The slight reduction in welding current, voltage and travel rate for Ti-15-3 welds produced in Phase II, which resulted in a slightly lower overall energy input to the weld zone, had a minimal effect on the beta grain structure observed in the autogenous welds. Figures 8A–C show the top and bottom surfaces, and a through-thickness cross-section perpendicular to the welding direction, respectively, for the autogenous, control weld in Ti-6-4 sheet. The FZ beta grain morphology paralleled that of the autogenous weld in Ti-15-3, with the principal difference being a coarser columnar grain size (Table 2) and the occurrence of more discontinuous and narrow centerline beta grains. As the transverse section in Fig. 8C shows, much of the FZ was only two beta grains in thickness.

As with the control weld, the beta grain size and morphology of Ti-15-3 welds inoculated with Ti-6-4 powder in Phase II were similar to those produced in Phase I. Figures 9A–C show the top and bottom surfaces and transverse, through-thickness cross-section, respectively, for the GTA weld produced in Ti-6-4 sheet with Ti-6-4 powder inoculation. Although the beta grain size in the equiaxed region was not as refined as that observed in the inoculated Ti-15-3 welds (0.25 mm/0.098 in. vs. 0.15 mm/0.0059 in.) appreciable grain refinement was in evidence as compared to the control weld. In contrast to the Ti-15-3 welds, the locations of powder particles within the FZ microstructure were generally masked by a transformed-beta microstructure comprised of a mixture of fine, acicular alpha and/or alpha-prime martensite. Analysis of the weld top surface at increased magnification in Figs. 10A–C revealed an equiaxed beta grain morphology at the center of the FZ (Fig. 10A) and only occasional evidence of powder particles on the surface (Fig. 10B). Difficulties in identifying powder particles on the weld surface resulted from their nominally identical chemistry to that of the base metal and the migration of solidification grain boundaries to form equiaxed grains. Near the fusion boundary, which was difficult to precisely discern, occasional columnar-shaped grains were observed as shown in Fig. 10C.

The application of a reversing (3-Hz), 50-gauss longitudinal magnetic field visibly stabilized and "stiffened" the arc. With no powder additions, application of the magnetic field did not influence the columnar FZ morphology and grain size exhibited by the control welds. As quantitative results in Table 2 show, the combination of EMS with powder additions for both powder/base metal combinations reduced the grain refinement effectiveness in terms of both the equiaxed beta grain size and the proportion of equiaxed-to-columnar grains. This effect was most significant for the Ti-15-3 weld. Although the weld exhibited a reinforcement consistent with powder additions and welds produced without EMS, only occasional powder particles and equiaxed dendrites were observed on the top surface. The bottom side of the Ti-15-3 weld was essentially identical to that of the autogenous welds. The weld produced in Ti-6-4 with EMS and powder additions exhibited refinement on the top surface and through thickness, but a columnar grain structure on the bottom surface. Unfortunately, experimental limitations precluded direct observation of the weld pool to ascertain changes in weld pool fluid flow which may have promoted this decrease in effectiveness.

Three-point bend testing of longitudinal-weld-oriented specimens in Ti-6Al-4V sheet showed an average elongation for FZ crack initiation (two specimens per condition in as-welded condition) of 7.4% for the control weld, 7.9% for the weld produced only with powder, and 7.9% for the weld produced with a combination of powder and longitudinal magnetic field. An SEM examination of bend specimen fracture surfaces indicated a transgranular fracture mode through the weld FZ for both autogenous control welds (Figs. 11A and B) and for welds produced with powder additions (Figs. 11C and D); with the latter weld exhibiting a more faceted macroscopic appearance.

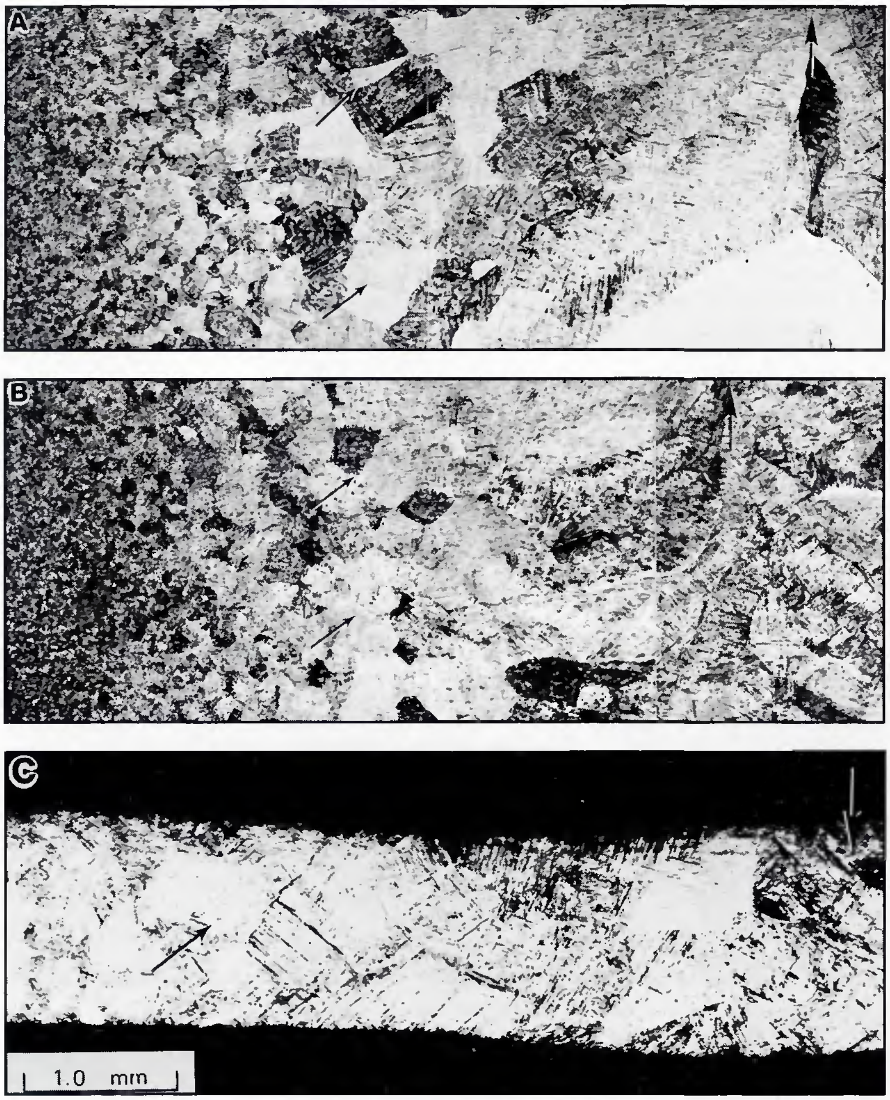

Fig. 8 — Light micrographs of autogenous GTA weld in Ti-6-4 sheet: A — top surface; B — bottom surface; C — transverse, through-thickness cross-section. Large arrows indicate FZ centerline and/or welding direction, small arrows indicate approximate fusion line.

Discussion

Results of the present investigation concurred with those of earlier experimental and theoretical studies (Refs. 21–24) in demonstrating the effectiveness of microcooler inoculation in inhibiting columnar grain growth and refining the FZ grain structure in GTA welded titanium sheet. More importantly, this study has provided specific information regarding solidification phenomena experienced during microcooler inoculation of titanium welds and evolution of the beta grain structure in the solid-state during weld cooling.

Examination of the solidification substructure in the inoculated Ti-6-4 powder/Ti-15-3 sheet welds clearly revealed the nucleation of equiaxed dendrites directly upon partially melted powder particles in the FZ, with the extent of this nucleation greatest near the top of the FZ. As indicated earlier, the proportion of added powder particles which survived to ultimately serve as grain nuclei was quite low, with the majority of the particles melting and thereby lowering the temperature and reducing temperature gradients near the trailing edge of the weld pool. The subsequent growth of equiaxed dendrites in the vicinity of the trailing edge of the weld pool effectively inhibited columnar grain growth often to less than 15% of the top surface width and precluded formation of longitudinal centerline grains. In the center and bottom regions of the FZ, a much lower density of powder particles was visible and similarly provided nucleation sites for equiaxed-dendritic grains. The presence of equiaxed grains without evidence of powder particles indicates that additional grains grew from dendrite tips fragmented from equiaxed dendrites near the FZ surface. As indicated previously, such a mechanism has been previously proposed (Refs. 5, 6) for grain refinement in titanium welds solidified under the action of EMS. It may be apparent that sufficient natural convective fluid flow occurs in the weld pool to provide such fragmentation without EMS, particularly when considering the presence of numerous large equiaxed dendrites within the pool. The homogeneous nucleation of beta grains at supercooled "freezing centers," as proposed by Ivochkin (Ref. 22), seems unlikely due to requirements for high undercoolings and the greater likelihood of heterogeneous nucleation.

Within the limited ranges evaluated, the powder size and powder flow rate showed relatively little effect on the beta grain morphology or quantitative measurements of grain size. Welds produced with the coarse particles did show slightly greater refinement and, as expected, the survival of more powder particles within the FZ. Based on these results, it seems possible that a further increase in powder particle size could further increase particle stability and improve refinement at the bottom of the FZ. Indeed, the use by Soviet investigators (Refs. 24, 25) of appreciably larger microcooler particles suggests this possibility. The powder feed rate also showed only a minimal effect on quantitative grain refinement. Based on the results of this and previous work (Refs.

20, 21), it is suggested that sufficient powder should be added to provide a slight excess of loose, unincorporated powder on the weld pool surface, without degrading process stability. Obviously, the associated adherence of some of these powder particles and the formation of an irregular weld surface must be considered and appropriately addressed in fatigue-critical applications.

Difficulties in promoting the movement and survival of greater numbers of powder particles deeper into the weld pool, and thereby providing greater and more uniform grain refinement on the bottom of the weld FZ, represents the most significant limitation to this process, particularly with regard to its potential application to greater sheet thicknesses. As described earlier, Boldyrev, *et al.* (Refs. 24, 25), suggested that the simultaneous application of longitudinal field (400 gauss, 5 Hz) and the addition of Ti and Zr powder to GTA welds in titanium sheet provides superior grain refinement and weld properties vs. welds produced only with powder additions. He attributed these improvements to the manner in which EMS displaces powder particles to the solidification front in a more uniform and effective manner than only by natural convective fluid flow in the weld pool. However, his work provides very limited quantitative or qualitative analyses of grain refinement under these two conditions and no direct evidence or explanation for such an effect. In the present study, the simultaneous application of powder additions and EMS at a comparatively lower field strength and reversing frequency (50 gauss, 3 Hz), reduced the effectiveness of grain refinement. Although direct observation of the weld pool fluid flow was not possible, this reduction may have been attributed to EMS promoting a greater mixing of cooler liquid containing powder particles at the trailing edge of the weld pool with superheated liquid from the center of the weld pool. Such mixing would result in an increase in the liquid temperature and promote greater temperature gradients, and the survival of fewer particles to provide nuclei for equiaxed dendrites. Such conditions would also reduce the tendency for the formation of equiaxed dendrites via conventional mechanisms. Singularly, the application of a longitudinal field at low frequencies would be expected to promote circumferential fluid flow and thereby promote such removal of powder particles from the solid-liquid interface rather than their movement to this interface. In actuality, the nature of fluid flow in the weld pool under an intense, reversing magnetic field, and in combination and competition with natural convective fluid flow in the weld pool (including the effect of powder particles on this flow) would be very complex. It is suggested that the greater success of Boldyrev, *et al.*, with EMS and powder additions may be related to the larger, and therefore kinetically more stable, powder particle particles employed. Clearly, a more systematic, detailed analysis of exactly how powder size, feed rate, welding parameters and EMS influence fluid flow in the weld pool, and ultimately solidification phenomena, will be required in order to optimize grain refinement effects via microcooler additions.

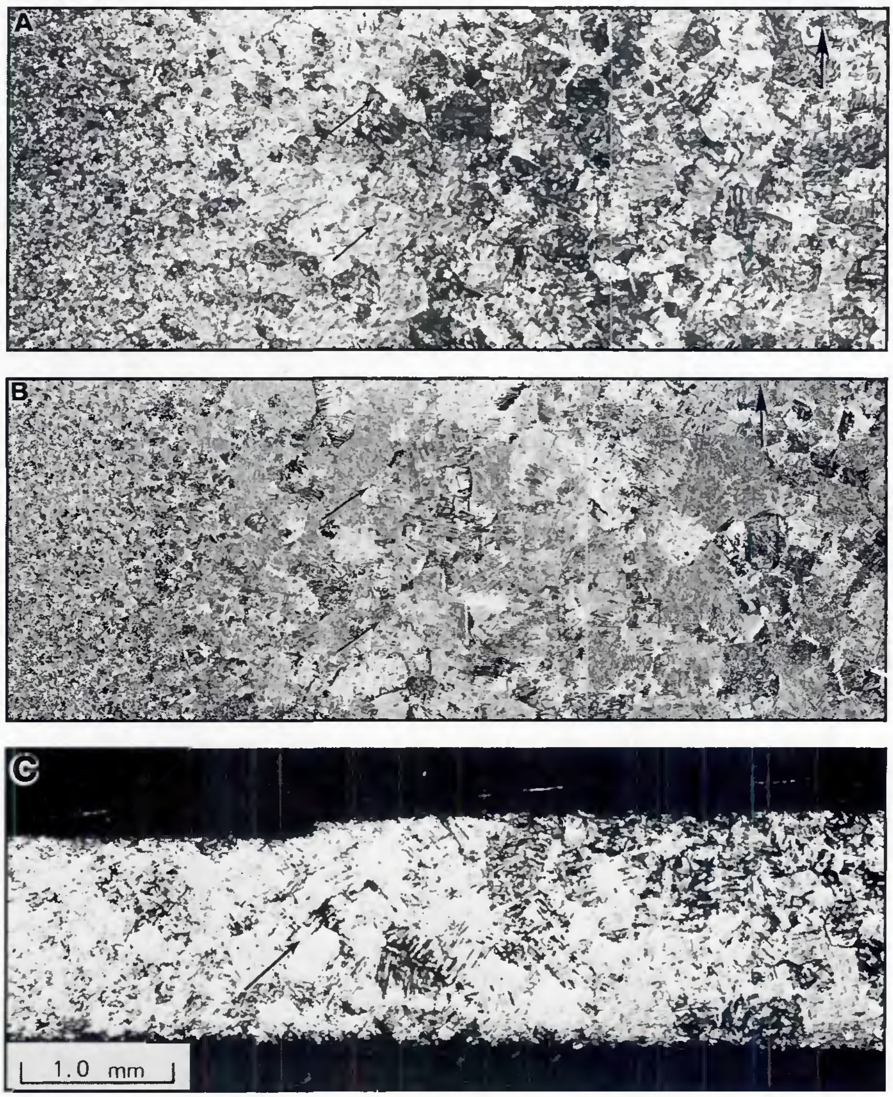

Fig. 9 — Light micrographs of GTA weld in Ti-6-4 sheet produced with addition of coarse-diameter Ti-6-4 powder at a rate of 0.055 g/min: A — top surface; B — bottom surface; C — transverse, through-thickness cross-section. Large arrows indicate FZ centerline and/or welding direction, small arrows indicate approximate fusion line.

Results of this study have shown that the room-temperature beta grain structure is also a strong function of solid-state phenomena that occur subsequent to weld solidification. Following solidification, the irregular solidification-substructure boundaries between equiaxed dendrites straighten and migrate in order to reduce their surface energy. Similar observations of such migration of large-angle grain boundaries away from the original solidification grain boundaries have been reported in other single-phase alloys, such as cupronickel alloys and austenitic stainless steels. As shown in Fig. 6B, there is little correlation between the migrated and original equiaxed-dendrite boundaries. The appreciably higher density of equiaxed grains vs. both powder particles and equiaxed dendrites, and the frequent presence of several fine equiaxed grains within a single equiaxed dendrite, also suggests the occurrence of a dynamic recystallization process during weld cooling. The extent of grain boundary migration and dynamic recystallization is dependent on alloy chemistry, with metastable-beta alloys generally more susceptible to such phenomena than alpha-beta alloys in part due to their lower beta transus temperature. Such differences may explain the finer equiaxed beta grain size observed in

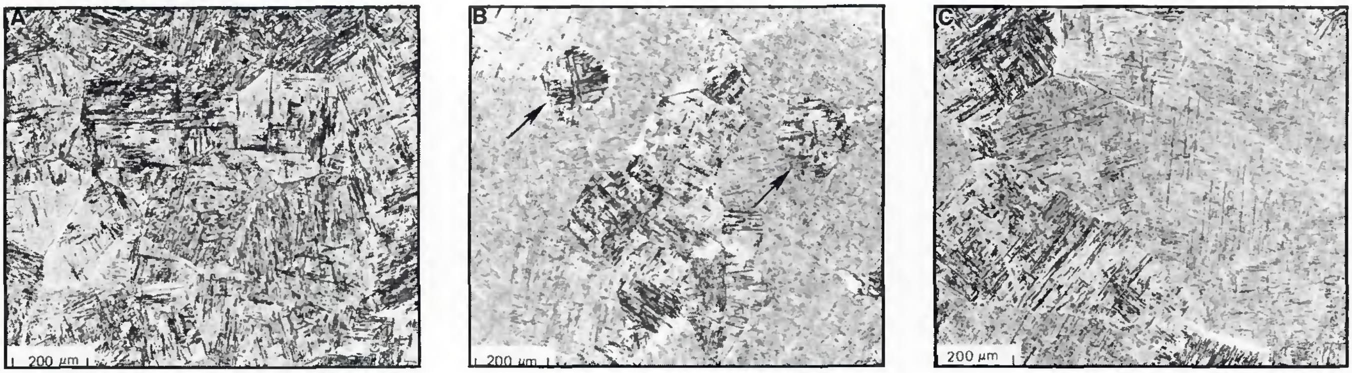

Fig. 10 — Light micrographs of GTA weld FZ top surface in Ti-6-4 sheet produced with addition of coarse-diameter Ti-6-4 powder at a rate of 0.055 g/min: A — fine, equiaxed beta grains at center of FZ; B — evidence of Ti-6-4 powder particles (arrows) within beta grains; C — columnar beta grain near fusion boundary.

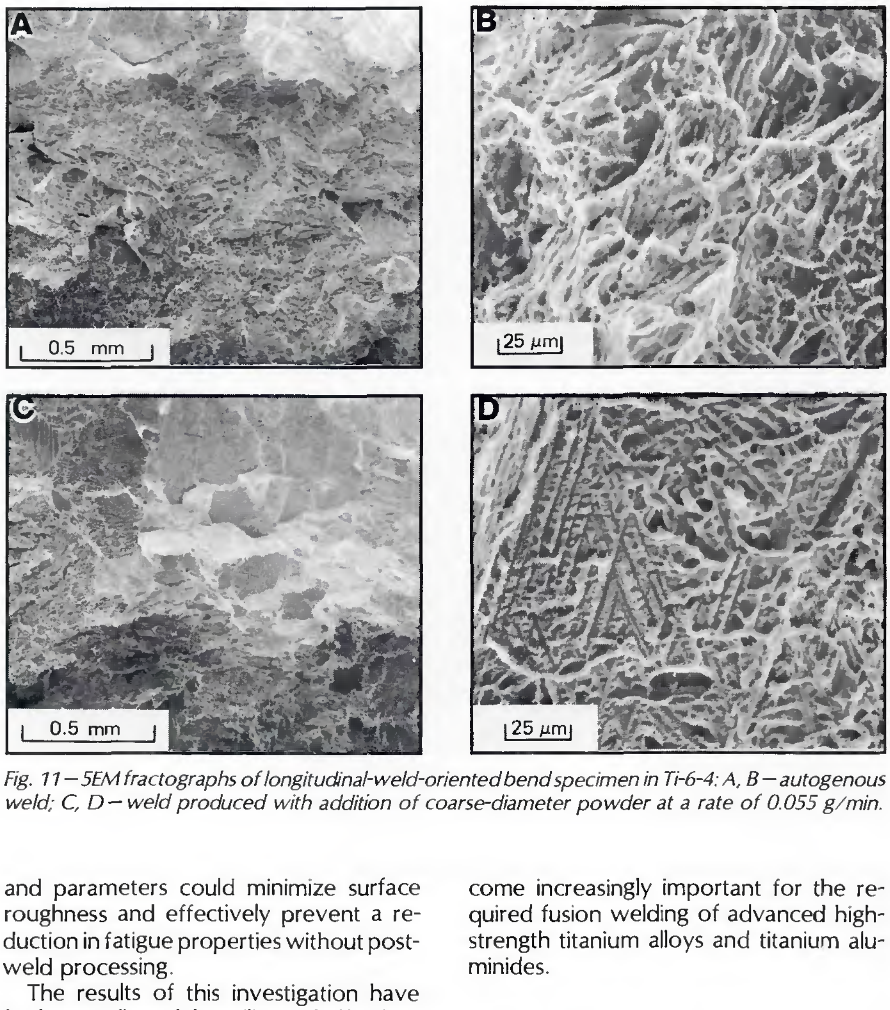

Fig. 11 — SEM fractographs of longitudinal-weld-oriented bend specimen in Ti-6-4: A, B — autogenous weld; C, D — weld produced with addition of coarse-diameter powder at a rate of 0.055 g/min.

Ti-15-3 vs. Ti-6-4.

It is important to note that evolution of the transformed-beta microstructure during weld cooling and/or postweld heat treatment, and the mechanical properties of the microstructures, will be dependent upon the morphology of this fine, migrated and/or recrystallized beta grain structure, not the original solidification beta grain structure. The absence of a significant influence of beta grain size and morphology on the bend ductility of GTA welds in Ti-6Al-4V sheet appeared to be related to the transgranular nature of fracture exhibited by these FZ structures. Certainly, transformed-beta FZ microstructures in many high-strength titanium alloys in which intergranular fracture occurs would be significantly influenced by such differences in FZ beta grain size and morphology.

The presence of fine pores or shrinkage cavities at the center of coarser powder particles must be considered as potentially reducing weld S-N fatigue properties. For welds produced in mill-annealed near-alpha or alpha-beta titanium alloys, in which the FZ yield strength is typically well above that of the base metal, the influence of occasional, extremely fine pores would not likely degrade S-N fatigue properties of the composite weldment. However, in heat-treated welds, or welds produced in metastable-beta titanium alloys in which the base metal and FZ strengths are similar, such porosity could promote premature fatigue crack initiation and degrade fatigue life. If such degradation is in fact observed, the use of finer powder particles that showed a lesser propensity for pore formation, or the utilization of particulate produced via alternate rapid-solidification or mechanical processes would be required. Irregularities on the as-welded FZ surface of welds experiencing appreciable powder particle adherence (as in Fig. 4) may likewise serve as fatigue crack initiation sites. Although FZ surfaces could be ground smooth, it is rather suggested that the further optimization of powder application techniques and parameters could minimize surface roughness and effectively prevent a reduction in fatigue properties without postweld processing.

The results of this investigation have further confirmed the utility and effectiveness of microcooler additions in refining the FZ grain structure of welds in titanium sheet. Obviously, appreciable further investigation is required to optimize the process and to obtain an improved understanding of how applied magnetic fields may enhance heterogeneous nucleation on the bottom of the FZ. The necessity to provide such refined beta grain structures, while maintaining relatively slow weld cooling rates to optimize the transformed-beta microstructure, will become increasingly important for the required fusion welding of advanced high-strength titanium alloys and titanium aluminides.

Conclusions

1) Significant grain refinement was achieved in the FZ of GTA welds in Ti-15-3 by inoculation with Ti-6-4 powder. Welds produced with powder additions exhibited fine, equiaxed grains throughout a large proportion of the FZ, in contrast to the coarse, columnar beta grains exhibited by the FZ of autogenous welds.

2) Metallographic analysis showed columnar beta grain growth to be effectively blocked by the heterogeneous nucleation

and growth of equiaxed dendrites throughout a large proportion of the FZ. Near the top of the FZ, and to a lesser extent in the central and lower FZ regions, equiaxed dendrites were observed to grow directly from partially melted powder particles. The presence of equiaxed dendrites in central and lower FZ regions nearly devoid of powder particles also suggested their growth from fragmented dendrite arms. It is proposed that the stability of these powder particles and dendrite fragments in the molten weld pool and equiaxed grain growth was afforded by the complete melting of a large proportion of the added powder particles which effectively reduced the liquid temperature and temperature gradients in the rear portion of the weld pool.

3. The beta grain structure present at room temperature, which would ultimately influence FZ mechanical properties, differed appreciably from the solidification grain structure due to grain boundary migration and possible dynamic recrystallization.

4. Powder additions to GTA welds in Ti-6-4 sheet also markedly reduced the FZ grain size, albeit to a somewhat lesser extent than observed in Ti-15-3. Grain refinement did not significantly influence the bend ductility of GTA welds in Ti-6-4. This was attributed to the principally transgranular mode of fracture observed in these welds upon which grain size had relatively little influence.

5. The combination of powder additions and EMS at moderate field strength resulted in less effective grain refinement vs. powder additions alone.

References

1. Baeslack, W. A. III, Becker, D. W., and Froes, F. H. 1984. Advances in titanium alloy welding metallurgy. *Journal of Metals* 36(5):46-58.

2. Savage, W. F. 1980. 1980 Houdremont lecture—Solidification, segregation and welding imperfections. *Welding in the World* 18(5,6):89-114.

3. Baeslack, W. A. III, and Mahajan, Y. 1979. Intergranular fracture of heat-treated weldments in a high-strength alpha-beta titanium alloy. *Scripta Metallurgica* 13:1.

4. Baeslack, W. A. III, and Banas, C. M. 1981. A comparative evaluation of laser and gas tungsten arc weldments in high-temperature titanium alloys. *Welding Journal* 60(7):121-s to 130-s.

5. Brown, D. C., Crossley, F. A., Rudy, J. F., and Schwarzbart, H. 1962. The effect of electromagnetic stirring and mechanical vibration on arc welds. *Welding Journal* 41(6):241-s to 250-s.

6. Boldyrev, A. M., Dorofeev, E. B., and Antonov, E. G. 1971. Controlled solidification during fusion welding. *Welding Production* 18(6):54-58.

7. Kuznetosov, D. V. 1972. Effect of electromagnetic agitation on the weld pool on the structure and properties of joints in VT6S alloy. *Welding Production* 19(5):14.

8. Shlenkov, G. M. 1974. The effect of electromagnetic stirring on the properties of welded joints in thin titanium sheet. *Welding Production* 21(12):34-37.

9. Blashchuk, V. E., and Shelenkov, G. M. 1976. Effect of electromagnetic agitation of weld pool on the properties of joints in VT 1-O alloy. *Automatic Welding* 29(8):29-31.

10. Shelenkov, G. M. 1979. The effect of electromagnetic stirring on the properties of welded joints in titanium alloy AT3. *Welding Production* 26(2)23-26.

11. Cherynsh, V. P., and Pakharenko, V. A. 1979. The kinetics of solidification of pool metal in welding with electromagnetic stirring. *Automatic Welding* 32(3):3-5.

12. DeNale, R., and Lukens, W. E. 1984. Effect of electromagnetic stirring on weld pools. *Proceedings of Ti-6211 Basic Research Program, Second Conference*, B. B., Rath, B. A. MacDonald and O. P. Arora, eds., Office of Naval Research, Arlington, Va., 1984, pp. 203-228.

13. Matsuda, F., Ushio, M., Nakagawa, H., and Nakata, K. 1979. Effects of electromagnetic stirring on the weld solidification structure of aluminum alloys, *Arc Physics and Weld Pool Behavior*, The Welding Institute, Cambridge, U.K., pp. 337-347.

14. Matsuda, F., Nakata, K., and Sano, N. 1986. Effect of electromagnetic stirring on weld solidification structure of austenitic stainless steels. *Transactions of the JWRI* 15(2):155-166.

15. Kou, S., and Le, Y. 1986. Nucleation mechanisms and grain refining of weld metal. *Welding Journal* 65(12):305-s to 313-s.

16. Abralov, M. A., Abdurakhmanov, R. U., and Iuldashev, A. T. 1978. The effect of electromagnetic action on the primary solidification of titanium. *Welding Production* 25(5):1-3.

17. Simpson, R. P. 1977. Controlled weld pool solidification structure and resultant properties with yttrium inoculation of Ti-6Al-6V-2Sn welds. *Welding Journal* 56(3):67-s to 87-s.

18. Misra, M. S., Olson, D. L., and Edwards, G. R. 1983. The influence of process parameters and specific additions on epitaxial growth in multiple pass Ti-6Al-4V welds. *Grain Refinement in Castings and Welds*, G. J. Abbaschian and S. A. David, eds., TMS/TIME pp. 259-274.

19. Nordin, M. C., Edwards, G. R., and Olson, D. L. 1987. The influence of yttrium microadditions on titanium weld metal cracking susceptibility and grain morphology. *Welding Journal* 66(11):342-s to 352-s.

20. Ivochkin, I. I. 1965. Suppression of columnar crystal growth by "freezing" the molten pool. *Welding Production* 12(12):1-3.

21. Shamanin, M. V. 1966. Suppression of columnar growth by feeding metal powder into the molten pool. *Welding Production* 13(10):40-42.

22. Boldyrev, A. M., Petrov, A. S., and Dorofeev, E. B., 1979. The effect of methods of weld pool modification on the mechanical and corrosion properties of welded joints in titanium alloy OT4-1. *Welding Production* 26(5):5-8.

23. Boldyrev, A. M., Petrov, A. S., and Dorofeev, E. B. 1983. Improving the impact strength of welds in OT4-1 alloy by adding zirconium. *Automatic Welding* 36(5):69-70.

24. Becker, D. W., and Baeslack, W. A. III. 1980. Property/microstructure relationships in metastable-beta titanium alloy weldments. *Welding Journal* 59(3):85-s to 92-s.

Acknowledgments

The authors are indebted to The Welding Research Council for provision of a grant-in-aid to support Ms. Diane Hallum during the performance of this work. Appreciation is also expressed to the Wright Research and Development Center, Wright-Patterson Air Force Base, Ohio, for providing the titanium powder and sheet.